Arthropod Structure & Development 61 (2021) 101012

Contents lists available at ScienceDirect

Arthropod Structure & Development

journal homepage: www.elsevier.com/locate/asd

Review article

The development and function of neuronal subtypes processing color and skylight polarization in the optic lobes of *Drosophila melanogaster*

Gizem Sancer, Mathias F. Wernet*

Freie Universität Berlin, Fachbereich Biologie, Chemie und Pharmazie, Institut für Biologie – Neurobiologie, Königin-Luise Strasse 1-3, 14195 Berlin, Germany

ARTICLE INFO

Article history:
Received 31 May 2020
Received in revised form
1 November 2020
Accepted 19 November 2020
Available online 19 February 2021

Keywords:
Neural circuits
Color vision
Skylight polarization vision
Neuronal cell types
Circuit assembly and function
Drosophila melanogaster

ABSTRACT

The retinal mosaics of many insects contain different ommatidial subtypes harboring photoreceptors that are both molecularly and morphologically specialized for comparing between different wavelengths versus detecting the orientation of skylight polarization. The neural circuits underlying these different inputs and the characterization of their specific cellular elements are the subject of intense research. Here we review recent progress on the description of both assembly and function of color and skylight polarization circuitry, by focusing on two cell types located in the distal portion of the medulla neuropil of the fruit fly *Drosophila melanogaster*'s optic lobes, called Dm8 and Dm9. In the main part of the retina, Dm8 cells fall into two molecularly distinct subtypes whose center becomes specifically connected to either one of randomly distributed 'pale' or 'yellow' R7 photoreceptor fates during development. Only in the 'dorsal rim area' (DRA), both polarization-sensitive R7 and R8 photoreceptors are connected to different Dm8-like cell types, called Dm-DRA1 and Dm-DRA2, respectively. An additional layer of interommatidial integration is introduced by Dm9 cells, which receive input from multiple neighboring R7 and R8 cells, as well as providing feedback synapses back into these photoreceptors. As a result, the response properties of color-sensitive photoreceptor terminals are sculpted towards being both maximally decorrelated, as well as harboring several levels of opponency (both columnar as well as intercolumnar). In the DRA, individual Dm9 cells appear to mix both polarization and color signals, thereby potentially serving as the first level of integration of different celestial stimuli. The molecular mechanisms underlying the establishment of these synaptic connections are beginning to be revealed, by using a combination of live imaging, developmental genetic studies, and cell type-specific transcriptomics.

1. Introduction

Despite its homogenous external morphology with ~800 unit eyes (ommatidia), the adult compound eye of the fly *Drosophila melanogaster* contains different ommatidial subtypes of that manifest specialization ideally suited for serving specific tasks (Kind et al., 2020). Tightly regulated expression of either one out of four different rhodopsin genes, as well as, in some cases, morphological differences in the ultrastructure of light-gathering rhabdomeric membranes of the central photoreceptors R7 and R8, together generate at least three subtypes of ommatidia (Fig. 1A): In the main part of the retina so-called 'pale' and 'yellow' subtypes are distributed randomly, yet in an uneven ratio of 35%–65%, which is conserved in larger fly species (Franceschini et al., 1981; Fortini and Rubin, 1990; Feiler et al., 1992; Bell et al., 2007; Hilbrant et al., 2014). Interestingly, pale R7 always express the *rh3* gene in, encoding the opsin moiety of the UV-sensitive pigment Rh3, which is paired with expression of the gene *rh5* in pale R8 photoreceptors of the same ommatidium, encoding the opsin moiety of the blue-sensitive pigment Rh5 (Chou et al., 1996; Papatsenko et al., 1997). In contrast, R7 cells in yellow ommatidia always contain another UV pigment (Rh4), whose sensitivity is slightly shifted to longer wavelengths, paired with a green-sensitive Rh6 pigment in yellow R8 (Huber et al., 1997; Chou et al., 1999; Salcedo et al., 1999). Although the genetic mechanisms behind pale/yellow choice in R7 and R8 have been elucidated (Mikeladze-Dvali et al., 2005; Wernet et al., 2006; Jukam et al., 2013; Johnston and Desplan, 2014), the communication of these choices between R7 and R8 remains incompletely understood (Wells et al., 2017). Due to their different spectral sensitivities, pale and yellow photoreceptor subtypes are

* Corresponding author.
E-mail address: mathias.wernet@fu-berlin.de (M.F. Wernet).

https://doi.org/10.1016/j.asd.2020.101012

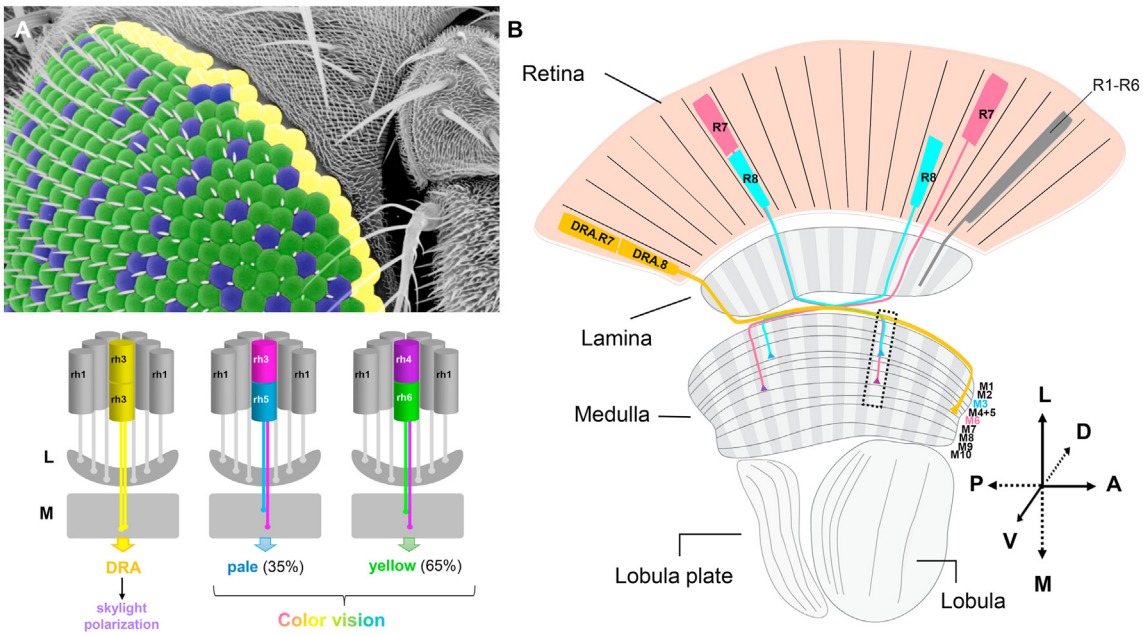

Fig. 1. Neural circuit elements processing color versus skylight information in the fly. (A) Top: Scanning electron micrograph depicting the distribution of three different ommatidial subtypes, false colored as blue (pale ommatidia), green (yellow ommatidia) and yellow (DRA ommatidia) in the adult *Drosophila* eye. Bottom: Schematic summarizing rhodopsin expression in these three ommatidial subtypes. Axons of inner photoreceptors R7 and R8 terminate in specific layers of the medulla neuropil (M). (L: Lamina, M: Medulla). (B) Schematic description of the *Drosophila* retina and the underlying optic lobe containing four neuropils: lamina, medulla, and lobula complex (comprised of lobula and lobula plate). A virtual section along the anterior–posterior axis is shown for a better visualization of the subdivision of the lobula complex. As a consequence, only one equatorial edge of the DRA is visible (yellow photoreceptors). Note that R7 and R8 photoreceptors from any given non-DRA ommatidium (shown in purple and cyan, respectively) terminate in different layers of the same medulla column (one example is shown as dashed box), whereas photoreceptors from neighboring ommatidia terminate in neighboring columns. This retinotopic organization is flipped due to a crossing over of axons in a chiasm. In contrast, axons of R1-6 photoreceptors (in gray) terminate in the lamina, without crossing over, where they wire according to the complex 'neural superposition' pattern (Langen et al., 2015).

perfectly suited to extract different kinds of spectral comparisons from the visual environment (Salcedo et al., 1999). Furthermore, behavioral experiments as well as physiological studies have confirmed that the pale/yellow mosaic is crucial for mediating *Drosophila* color vision (Yamaguchi et al., 2010; Schnaitmann et al., 2013; Melnattur et al., 2014; Schnaitmann et al., 2018; Heath et al., 2019). The occurrence of the third ommatidial subtype is always restricted to one or two rows of ommatidia along the dorsal rim of the eye, hence called 'dorsal rim area' (DRA) (Wada, 1974; Labhart and Meyer, 1999; Tomlinson, 2003; Wernet et al., 2003). Only in DRA ommatidia, R7 and R8 are monochromatic and therefore not suitable for directly comparing spectral information, as they both express the same UV sensitive pigment Rh3 (Fortini & Rubin, 1990, 1991). However, like in many other insect species, DRA.R7 and DRA.R8 are specialized to detect the angle of polarized skylight due to the strict alignment of opsin molecules along their untwisted rhabdomeric membranes (Smola and Tscharntke, 1979; Wunderer and Smola, 1982; Wernet et al., 2012). Rhabdomeres of R7 vs R8 from the same ommatidia form orthogonal analyzers (Wernet et al., 2012), whereas analyzer directions of neighboring DRA ommatidia gradually change along the DRA, forming a fan-shaped array of skylight polarization detectors (Weir et al., 2016). In the DRA, R7 and R8, therefore, detect a separate modality of light (i.e. skylight polarization) and compare orthogonal angles of polarized light instead of different wavelengths. Indeed, even a behavioral generalist like *D. melanogaster* is able to keep stable headings over long periods of time (Coyne et al., 1982; Coyne et al., 1987; Dickinson, 2014), and its navigation skills using polarized light have been confirmed both under the real sky (Weir and Dickinson, 2012), as well as when walking (Wernet et al., 2012; Velez et al., 2014a, 2014b), or flying under laboratory conditions (Wolf et al., 1980; Mathejczyk & Wernet, 2017, 2019, 2020; Warren et al., 2018; Warren et al., 2019). Just like for pale and yellow ommatidia, the genetic mechanisms specifying DRA ommatidia have been elucidated (Wernet et al., 2003, 2014; Wernet and Desplan, 2014), resulting in a complete understanding of how the retinal mosaic of flies is patterned (Wernet et al., 2007), some of which are evolutionary conserved (Wernet et al., 2015; Perry et al., 2016).

The different kinds of visual information collected by these different ommatidial subtypes are transmitted to the optic lobes for further processing (Meinertzhagen and Hanson, 1993). The optic lobes in *Drosophila* consist of four successive, retinotopically organized neuropils called lamina, medulla, and the lobula complex, which is composed of lobula and lobula plate (Ito et al., 2014; Fischbach and Dittrich, 1989) (Fig. 1B). Photoreceptors R7 and R8 send axons directly to the medulla which is the most complex neuropil of the optic lobe with more than 80 different cell types and ~40,000 neurons (Fischbach and Dittrich, 1989). Many of these neurons occur once in every retinotopic column (hence ~800 times per optic lobe), which corresponds to the visual field of single ommatidia from the adult eye (columnar neurons), while other neuron types occur at fewer numbers while innervating many columns (multicolumnar neurons). Via precise synaptic connectivity, the columnar organization of the optic lobes ensures that retinotopy is maintained as information flows from the eye to higher brain regions. Usually, each neuron type also stratifies in specific medulla layers (named M1–M10, from distal to proximal) (Fischbach and Dittrich, 1989). The axons of pale and yellow R7 and R8 photoreceptors terminate in layers M6 and M3, respectively (Fischbach and Dittrich, 1989). Only in the DRA, both R7 and R8 terminate in the same deeper layer M6, yet R8 still terminating slightly more distally (Fischbach and Dittrich, 1989; Pollack and Hofbauer, 1991; Chin et al., 2014; Sancer et al., 2019) (Fig. 2). Despite several studies systematically characterizing both

morphology and connectivity of specific cell types in the optic lobes (Takemura et al., 2008; Tuthill et al., 2013; Nern et al., 2015; Takemura et al., 2015; Wu et al., 2016), relatively little is known about the differences between those neural circuits processing color versus polarized light inputs. More specifically, our knowledge remains limited about the importance of similarities versus differences in circuit architecture within columns of different and similar subtype identity, as well as their organization of cell types into distinct layers for informing color versus polarized light vision. More recently, several studies have investigated the circuit structure and photoreceptor connectivity in medulla columns located in both pale and yellow (Karuppudurai et al., 2014; Carrillo et al., 2015; Tan et al., 2015; Lin et al., 2016; Schnaitmann et al., 2018; Courgeon and Desplan, 2019; Heath et al., 2019), as well as in the DRA (Sancer et al., 2019, 2020). Here we review recent progress on the description of both assembly and function of color and skylight polarization circuitry, by focusing on two cell types that are photoreceptor targets located in the distal medulla of the *Drosophila* optic lobes, called Dm8 and Dm9 (Fischbach and Dittrich, 1989; Takemura et al., 2013).

2. Assembly and function color vision circuitry: lessons from Dm8 cells

In *Drosophila*, pale and yellow R7 cells (both UV-sensitive), pale R8 (blue-sensitive), and yellow R8 (green-sensitive) serve as detectors for color vision (Salcedo et al., 1999; Gao et al., 2008; Yamaguchi et al., 2010; Schnaitmann et al., 2013, 2018). Beyond the spectral sensitivity of these photoreceptors, it is crucial to understand the computations executed by the downstream network for the comparison of chromatic information (Song and Lee, 2018; Schnaitmann et al., 2020). Using behavioral assays like UV-versus-green spectral preference tests, fruit flies were shown to be strongly attracted to UV light (Gao et al., 2008; Otsuna et al., 2014). This is probably due to the fact that many insects interpret UV light as a celestial cue, since the spectrum of the open sky is richer in UV (when compared to direct sunlight) (Wehner, 2001). Hence, such responses to UV light thereby potentially inform innate escape responses. Systematic genetic screens revealed that this behavior is mediated by UV-sensitive R7 cells (both pale and yellow), as well as an amacrine-like cell in distal medulla (Dm) named Dm8 that is directly postsynaptic to R7 (Fischbach and Dittrich, 1989; Gao et al., 2008; Karuppudurai et al., 2014; Nern et al., 2015; Takemura et al., 2015). Cell type specific synaptic silencing of Dm8 cells in combination with rescue experiments for restoring their synaptic input cell type specifically revealed that this cell type is indeed necessary and sufficient for mediating UV spectral preference (Gao et al., 2008). A detailed analysis of Dm8 morphology revealed prominent lateral arborizations within the M6 layer, i.e. the target layer of R7 photoreceptors (Fischbach and Dittrich, 1989; Gao et al., 2008). Furthermore, studies using light microscopy and serial EM reconstruction showed that one Dm8 cell receives inhibitory synaptic input from R7 photoreceptors in ~13 adjacent ommatidia (Karuppudurai et al., 2014; Takemura et al., 2015), using histamine as neurotransmitter (Stuart, 1999). Therefore, synaptic connections suggest that one given Dm8 cell pools UV information from these adjacent columns. On the output side, Dm8 then conveys this pooled information to a columnar transmedullary cell

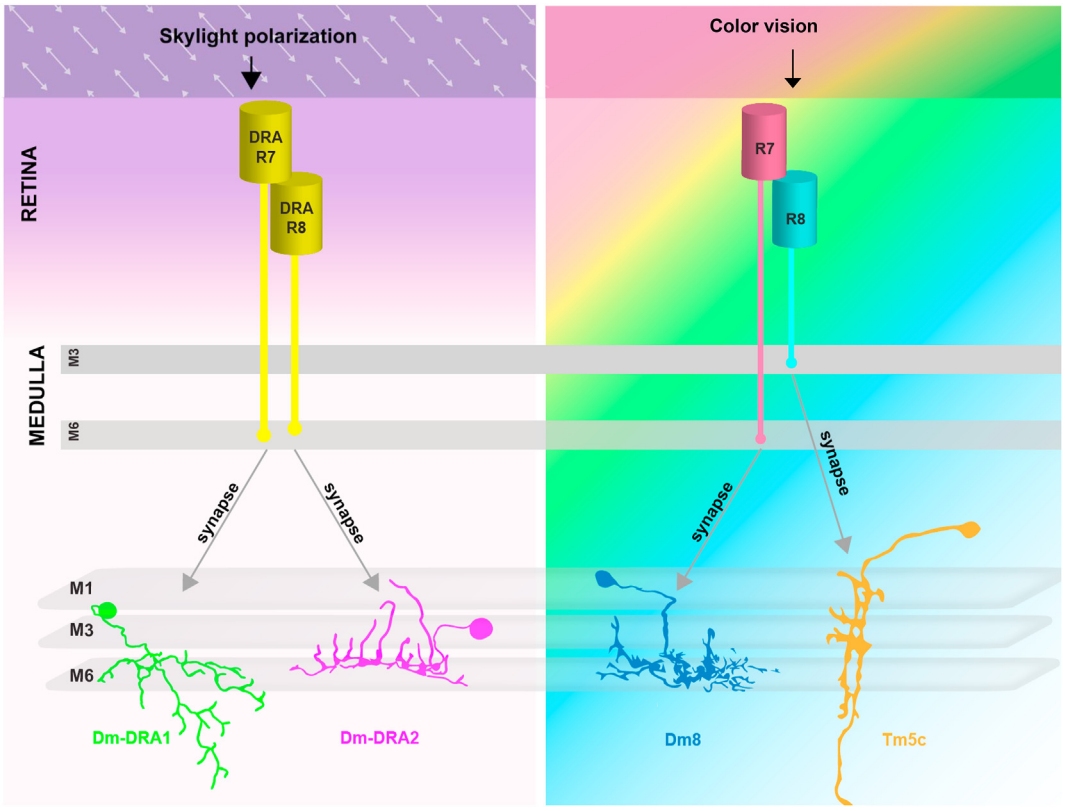

Fig. 2. Similarities and differences between medulla circuitry processing skylight polarization versus color. A graphical summary of the early circuit elements processing skylight polarization versus color vision. Polarization-sensitive DRA.R7 and DRA.R8 project axons to the same deep layer (M6) of the medulla, where they are connected to different postsynaptic partners, the horizontal cell types Dm-DRA1 and Dm-DRA2, respectively. Non-DRA R7 and R8 detect different wavelengths and project to different layers, where only R7 connects to the horizontal cell type Dm8 within layer M6, whereas R8 connects to the columnar cell typeTm5c in layer M3. Adapted from Sancer et al. (2019).

named Tm5c via an excitatory glutamatergic connection located in its center (Karuppudurai et al., 2014). When glutamatergic synaptic output of Dm8 cells is blocked or the expression of Kainate (glutamate) receptors is knocked down in Tm5c cells, flies show a reduced UV preference, suggesting that this circuit including an excitatory connection between Dm8 and Tm5c is important for UV preference (Karuppudurai et al., 2014). Remarkably, Tm5c also receives direct columnar input from blue- or green-sensitive R8 cells thereby completing the minimal architecture of the circuit mediating spectral preference and color vision (Meinertzhagen et al., 2009; Karuppudurai et al., 2014) (Fig. 3A).

In order for this circuit to function properly, both dendritic size of Dm8 cells, as well as distribution of synapses across this field needs to be regulated during development. To ensure this, the R7 photoreceptors play an important role in the determination of the dendritic branch size of their Dm8 targets. They provide the morphogen Activin which acts through its receptor Baboon expressed in Dm8 to limit the development of arborizations and thereby restricting the dendritic field size of their respective postsynaptic partner (Ting et al., 2014). While its limitation is controlled by the presynaptic partner of Dm8, the growth of the dendritic field size is controlled via a separate mechanism: A recent study identified an important role for the lamina cell type L5, which projects axons into the medulla but is a not synaptically connected to either photoreceptors or to Dm8 (Luo et al., 2020). During early developmental stages, L5 cells provide an insulin like peptide (called DILP2) signal to the nearby Dm8 cells which has a facilitating effect on the dendritic expansion of Dm8 cells. In combination, antagonistic regulatory inputs via DILP2 (from L5) and Activin (from R7) together regulate the stereotyped morphology of Dm8 dendrites, presumably in order to ensure accurate dendritic size for proper circuit function (Luo et al., 2020).

Interestingly, synaptic inputs from R7 onto Dm8 are not evenly distributed along the Dm8 cell surface. In the center of most Dm8 cells a prominent dendritic projection extending distally from M6, reaching all the way into layers M4. This prominent protrusion defines the so-called 'home column' of a given Dm8 cell (Fischbach and Dittrich, 1989; Carrillo et al., 2015; Nern et al., 2015; Tan et al., 2015; Courgeon and Desplan, 2019; Menon et al., 2019). Although lateral branches of any given Dm8 can contact ~13 R7 terminals in layer M6, the Dm8 vertical protrusion contains an unproportionally high number of synapses, formed with the R7 occupying the home column (Takemura et al., 2015; Menon et al., 2019). While lateral branches of neighboring Dm8 cells overlap extensively, their home columns tile in the medulla, thereby providing Dm8 cells with both unicolumnar and multicolumnar attributes (Nern et al., 2015; Tan et al., 2015). As a result, almost every medulla column is home to one dedicated Dm8 cell (Takemura et al., 2015). Since Dm8 cells show strict preference for forming synapses with the R7 cell in their home column, the question was raised whether Dm8 cells also fall into specific pale- and yellow-specific subtypes. Recent developmental studies focusing on the cell-type specific expression of cell surface molecules revealed that such Dm8 subtypes indeed exist (Courgeon and Desplan, 2019). Further investigations then focused on how they could be matched with R7 pale and yellow subtypes (Carrillo et al., 2015; Tan et al., 2015; Courgeon and Desplan, 2019; Menon et al., 2019). Pale and yellow fates are stochastically determined in R7 cells during development (Wernet et al., 2006; Johnston and Desplan, 2014), through the evolutionarily-conserved expression of the transcription factor Spineless (Perry et al., 2016). Therefore, it seemed hard to imagine how the Dm8 cells of each medulla column would assume their pale/yellow identity before contacting its future presynaptic partner. Important insight came from the finding that matching pairs of cell surface molecules are

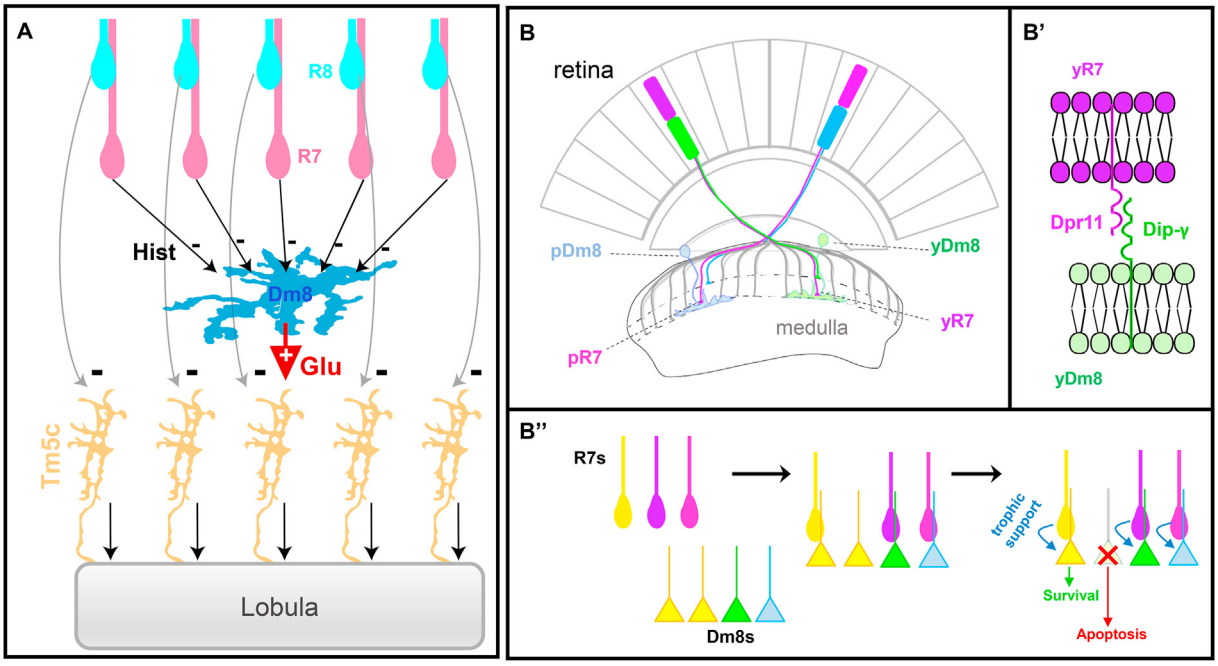

Fig. 3. Connectivity and circuit assembly of color-sensitive Dm8 cells. (A) The amacrine-like Dm8 cell receives inhibitory histaminergic inputs from ~13 neighboring R7 photoreceptors and provides excitatory glutamatergic input to the columnar Tm5c neuron which also receives direct photoreceptor inputs from R8 (Adapted from Karuppudurai et al. (2014)). (B) Pale and yellow R7 cells are connected to different Dm8 subtypes (pDm8 or yDm8). Pairing is controlled by the complementary cell adhesion molecules Dpr11 and DIP-γ expressed specifically in yR7 and yDm8, respectively (B′). Summary of a proposed mechanism that allows correct pairing between R7 subtypes and their specific post-synaptic targets: Different Dm8 subtypes are produced in excess independent of R7 subtypes. When correct R7 and Dm8 subtypes match, interaction leads to a trophic signal (for instance via Dpr-DIP) ensuring the survival of the Dm8 cell, whereas unmatched Dm8s are eliminated via apoptosis. Adapted from Courgeon and Desplan (2019).

expressed in yellow R7 cells and the Dm8 cells that they are synaptically connected to: the immunoglobin family cell member Dpr11 is expressed in yellow R7, whereas one of its specific binding partners called DIP-γ (for interacting partner gamma, another immunoglobulin transmembrane protein) is expressed in a distinct population of Dm8 cells, long before synapses are formed (Carrillo et al., 2015; Courgeon and Desplan, 2019; Menon et al., 2019). It turns out that two Dm8 subtypes (DIP-γ positive and DIP-γ negative) are produced in excess during development, originating from distinct neural progenitors (Courgeon and Desplan, 2019). In each medulla column, these subtypes then appear to compete for presynaptic R7 partners. When a yellow R7 photoreceptor terminal encounters a DIP-γ positive Dm8, interaction between Dpr11 and DIP-γ promotes the survival of this Dm8, whereas unmatched Dm8 subtypes are eliminated by apoptosis (Courgeon and Desplan, 2019). Therefore, excess production of alternative postsynaptic partners and target derived trophic support via DIP/Dpr cell surface molecules provide an elegant molecular mechanism for ensuring correct matching between stochastically specified presynaptic elements (yellow R7) and their prospective postsynaptic partners (DIP-γ or yellow Dm8) (Fig. 3B).

3. Modality-specific circuit elements for processing skylight polarization

Like in many other insects, the rhabdomeres of R7 and R8 cells residing in the DRA region of the adult eye form an orthogonal analyzer pair morphologically and molecularly specialized for detecting the celestial polarization pattern (Wunderer and Smola, 1982; Labhart and Meyer, 1999; Labhart and Wehner, 2006; Wernet et al., 2012). These two photoreceptors, therefore, produce similar yet opponent outputs. Little is known about how these polarization-opponent signals are processed by cell types in the DRA columns of the medulla of any insect (Labhart, 1988; el Jundi et al., 2011). Two studies recently investigated this by comparing the photoreceptor and Dm8 morphology between the columns of the DRA and the remaining medulla (Sancer et al., 2019, 2020). Interestingly, DRA.R8 morphology is rather unique, differing from non-DRA counterparts not only in Rhodopsin expression (expressing the R7 UV-Rhodopsin Rh3) and layer targeting (axons terminating in the R7 layer M6), but also in the distribution of its presynaptic sites, which resembles that of normal R7 cells (Sancer et al., 2019). Based on all these features, it appears that R8 photoreceptors in the DRA assume an R7-like fate, which is well in line with their function: to provide an orthogonal analyzer channel to DRA.R7 cells of equal weight (Sancer et al., 2019). The synaptic output of both R7-like photoreceptors within the same medulla layer M6 raises two central questions regarding the downstream network: First, are both DRA.R7 and DRA.R8 connected to the same Dm8 cell(s), despite having orthogonally opponent analyzer directions? And second, since one Dm8 cell usually pools from ~13 neighboring ommatidia – do Dm8 cells in the DRA integrate both polarization and color information? Indeed, a significant difference in the Dm8 morphology has recently been found between the DRA and non-DRA columns (Sancer et al., 2019). Since *Drosophila* optic lobe cell type nomenclature is based mostly on unambiguous morphological classification, this Dm8-like distal medulla cell in the DRA was renamed Dm-DRA1. Importantly, this new cell type exclusively receives DRA inner photoreceptor inputs, while avoiding contacts from color sensitive R7 photoreceptors (Sancer et al., 2019; Courgeon and Desplan, 2019). As a result, lateral arborizations of Dm-DRA1 cells reaching towards the center of the medulla were restricted to a more proximal sublayer within layer M6 (Fischbach and Dittrich, 1989), an identifying feature of Dm-DRA1 cells previously termed 'deep projections' (Fig. 4A) (Sancer et al., 2019). Importantly, the columnar sites of Dm-DRA1 photoreceptor contacts never overlapped with the dendritic fields of color sensitive Dm8 cells (Fig. 4A′ and A″). Since Dm-DRA1 cells heavily overlapped amongst their own kind (as Dm8 cells do amongst themselves), the DRA/non-DRA boundary is in fact the only place in the medulla neuropil where Dm8-like cells do not overlap, thereby reflecting a modality-specific boundary between color and polarization-sensitive inputs (Sancer et al., 2019).

Despite these differences, developmental studies suggest that Dm-DRA1 and Dm8 cells share a similar developmental origin (Courgeon and Desplan, 2019), hence Dm-DRA1 can probably be considered a third kind of 'true' Dm8 cells (in addition to DIP-γ positive and negative Dm8s). Unexpectedly, a second Dm8-like cell type was described in the M6 layer only in DRA medulla column which is morphologically different from Dm-DRA1 and was therefore named Dm-DRA2 (Sancer et al., 2019). All the arborizations of these cells were restricted to DRA columns hence not forming 'deep projections' while instead forming very prominent and characteristic vertical projections that are in close contact with photoreceptor axon terminals (Fig. 4B). Photoreceptor contacts of this second Dm8-like cell type also never overlapped with pale or yellow Dm8 cells and therefore represented a second kind of modality specific cell type for processing skylight information (Fig. 4B′ and B″). Interestingly, both Dm-DRA1 and Dm-DRA2 cell types overlap heavily with their own kind as well as between types, along the entire DRA (Sancer et al., 2019). However, Dm-DRA1 and Dm-DRA2 located at the same position stratify within slightly different layers within M6 (Dm-DRA1 always being located proximally of Dm-DRA2) (Fig. 4C). In fact the distance between them exactly matches the distance DRA.R7 and DRA.R8 axon termination sites within M6 (Sancer et al., 2019). The possibility of Dm-DRA1 and Dm-DRA2 being specific postsynaptic partners of DRA.R7 and DRA.R8, respectively, was indeed confirmed via molecular genetic tools, like GFP reconstitution across synaptic partners (GRASP) (Feinberg et al., 2008; Macpherson et al., 2015) and by using the trans-synaptic tracer tool trans-tango (Talay et al., 2017; Sancer et al., 2019). Therefore, only in the DRA region of the medulla neuropil (MEDRA), both R7 and R8 cells are synaptically connected to different subtypes of morphologically distinct Dm8-like subtypes, further supporting the observation that DRA.R8 cells become R7-like both in function and circuitry, when processing polarized skylight information.

The fact that Dm-DRA1 and Dm-DRA2 stratify in close proximity within two M6 sublayers of M6 while being connected to different presynaptic partners (DRA.R7 versus DRA.R8) raises the question how such synaptic specificity is achieved during development. So far, no immunoglobulin proteins are known to be specifically expressed in DRA circuit elements. Important insight into a possible mechanism facilitating the formation of specific synaptic connections in close proximity was gained by performing intravital imaging of sparsely labeled inner photoreceptor terminals as they grow into their medulla target layers (Sancer et al., 2019). Non-DRA R7 growth cones target swiftly to M6, whereas R8 growth cones pause at the distal end of the medulla (M0) and then actively extend towards M3 (Ting et al., 2005; Ozel et al., 2015). Although in adult DRA.R8 become more R7-like, developmental dynamics of DRA.R8 remain "normal R8" until mid-pupal stages. As a result, DRA.R8 axon terminals reach layer M6 at a later time point during the development, which might enable a temporal separation for synaptic partner choice (Fig. 4D). Certainly, specific expression of cell surface molecules might still play an important role, and more live imaging is needed to get a better understanding of how partner choice and transient cell–cell contacts influence the generation of synaptic specificity in the DRA.

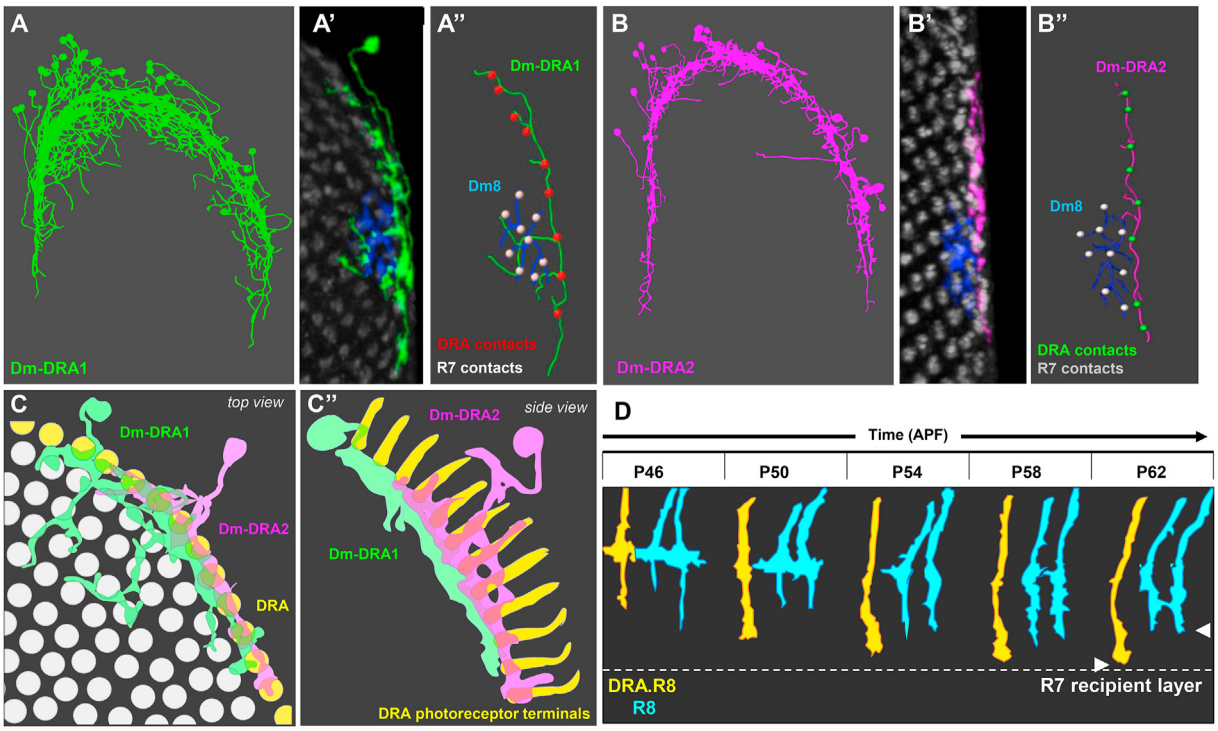

Fig. 4. Modality-specific Dm8-like cells processing skylight polarization. (A) Virtual assembly of multiple Dm-DRA1 clones along the DRA region of the medulla (MEDRA). Neighboring MCFO clones of a Dm-DRA1 cell (green) and a color sensitive Dm8 cell (blue) in A′. These two cell types never share photoreceptor contacts, as visible from their skeletons: Dm8-R7 contacts (gray spheres) and Dm-DRA1-DRA photoreceptor contacts (red spheres) in A″. (B) Virtual assembly of multiple Dm-DRA2 clones along the DRA of the medulla. Neighboring MCFO clones of a Dm-DRA2 cell (magenta) and a color sensitive Dm8 cell (blue) in B′. Again, these two cells never share photoreceptor contacts, as visible from their skeletons: Dm8-R7 contacts (gray spheres) and Dm-DRA2-DRA contacts (green spheres) in B″. (C) Two adjacent Dm-DRA cell clones of different subtypes (Dm-DRA1: green; Dm-DRA2: purple) located at the location along the anterior–posterior axis of the DRA (yellow circles). (C″): side view. Note the slight difference in sublayer stratification along the dorsoventral axis. (D) Illustration summarizing the developmental layer targeting of DRA.R8 (yellow) and non-DRA R8 (cyan) growth cones from 46 h after pupa formation (APF, P46) to 62 h APF (P62). Arrowheads point to layers M3 and M6, respectively. All data adapted from Sancer et al. (2019).

4. An additional layer of inter-ommatidial integration: Dm9 cells

In most cases, true color vision involves color opponent elements collecting information from at least two distinct chromatic channels (Longden, 2018). In recent years it became clear that in *Drosophila*, color opponency already starts at the level of photoreceptor terminals: Ultrastructural studies revealed that color-sensitive R7 and R8 photoreceptor terminals from the same ommatidium are bidirectionally synaptically connected to each other (Takemura et al., 2008, 2015). More recently, functional imaging of R7 and R8 terminals using cell-type specific expression of genetically encoded indicators of activity revealed short-UV/blue opponent signals in pale columns and long-UV/green opponency in yellow columns (Schnaitmann et al., 2018). This intra-ommatidial color opponency was shown to depend on direct reciprocal inhibition mediated by a specific isoform of a histamine gated chloride channel expressed rather specifically in inner photoreceptor terminals (while being absent from most inner photoreceptor target cells in the optic lobe) (Tan et al., 2015; Davis et al., 2020). In addition to this direct reciprocal intra-ommatidial inhibition, it has been suggested that medulla neurons expressing another histamine gated chloride channel isoform (called Ort) also provide feedback inhibition to photoreceptors (Schnaitmann et al., 2018). Hence, the outputs of histaminergic inner photoreceptors R7 and R8 are already opponent in nature, which must be taken into account when interpreting the functional properties of the cholinergic R7 → Dm8 → Tm5c circuit described above.

One recent study offered important new insight into the cellular mechanism providing feedback inhibition into R7 and R8 photoreceptor terminals. In fact, this study also revealed that inter-columnar interactions between neighboring ommatidia play an important role in shaping the color sensitive responses of R7 and R8 terminals (Heath et al., 2019). Once again, functional imaging of the photoreceptor terminals was used to reveal that neighboring columns provide additional (indirect) inhibitory input. For instance, inhibition is observed for blue-sensitive pale R8 terminals when stimulating with longer wavelengths, suggesting that yellow R8 photoreceptor input from neighboring ommatidia also shapes pale R8 output. Such inter-columnar inhibition could only be provided by horizontal cell types that contact several medulla columns, while also providing synaptic input into the photoreceptor terminals. The distal medulla cell type Dm9 was identified as the likely candidate, each cell spanning seven columns on, tiling in layers M2–M5 while overlapping in M1 and M6 (Fig. 5A) (Takemura et al., 2013; Nern et al., 2015). More importantly, Dm9 is the only medulla cell type that both receives synaptic input from R7 and R8 while also providing strong synaptic feedback onto both photoreceptor terminals (Fig. 5B) (Uhlhorn and Wernet, 2020). Indeed, functional imaging of R7 and R8 axon terminals, while silencing the synaptic output of Dm9 cells, specifically led to a disappearance of inter-ommatidial inhibition (Heath et al., 2019). Strikingly, Dm9 was shown to be both necessary and sufficient for mediating inter-ommatidial antagonism and thereby enabling additional color comparisons (Fig. 5C). Hence, this dual opponent system via intra-columnar and inter-columnar inhibition provides an efficient

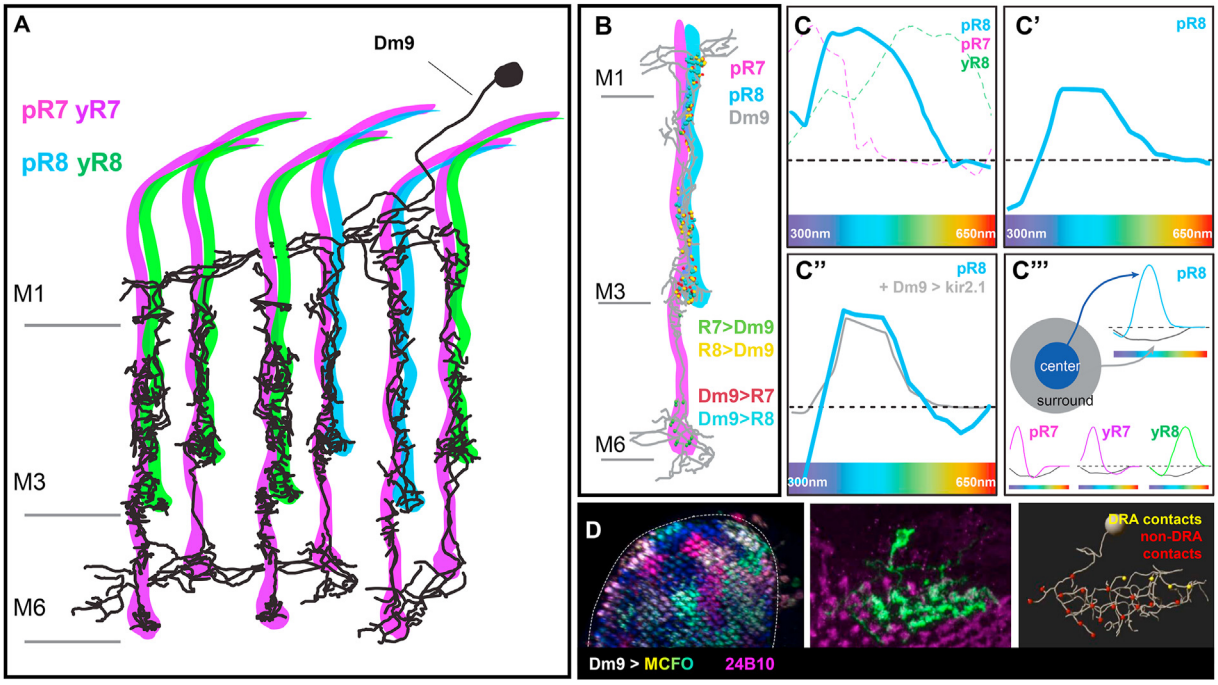

Fig. 5. Inter-ommatidial integration via Dm9 cells. (A) Skeleton of a Dm9 cell (black), covering multiple 'pale' and 'yellow' columns, where blue-sensitive R8 cells are paired with UV-sensitive R7 (pale) or green-sensitive R8 with UV-sensitive R7 (yellow), respectively. Inter-ommatidial connections of Dm9 and photoreceptors (and vice versa) exist in medulla layers M1 and M6. (B) Intra-ommatidial connections of Dm9 and photoreceptors are distributed from M1 to M6. Feedback synapses from Dm9 onto R7 and R8 (red and light blue, respectively) and R8 synapses onto Dm9 (yellow) locate between medulla layer M1 to M3, while R7 to Dm9 synapses (green) exist mainly within layer M6. (C) Uncoupled tuning curve of a 'pale' R8 photoreceptor (blue). A black dashed line depicts the baseline activity of 'pale' R8. Pink and green dashed lines show tuning curves of uncoupled 'pale' R7 and 'yellow' R8, respectively. (C′) Tuning curve of a 'pale' R8 photoreceptor when paired with 'pale' R7 of the same column: Intra-ommatidial inhibition is observed at short wavelengths. (C″) Tuning curve of a 'pale' R8 photoreceptor in a wild-type background reveals additional inter-ommatidial inhibition at longer wavelengths. The gray line depicts the same tuning curve after Dm9 inactivation. (C‴) Spectral filtering model for inner photoreceptors: Modeled output for predicted 'pale' R8 (blue) in the center and their surround over different wavelengths is shown. The modeled outputs for 'pale' R7 (pink), 'yellow' R7 (purple) or 'yellow' R8 (green) are shown below. All data adapted from Heath et al. (2019) and Uhlhorn and Wernet (2020). (D) Single cell morphology of a Dm9 cell, (E) Multi-Color Flp-Out (MCFO) clones of Dm9 cells tiling across the medulla. Lateral view of a Dm9 single-cell clone (green) located at the dorsal rim of the medulla. Skeleton of the same cell with DRA photoreceptor contacts shown in yellow and non-DRA contacts shown in red. Adapted from Sancer et al. (2020).

mechanism for 'sculpting' photoreceptor responses. Furthermore, consecutive modeling of color sensitive R7 and R8 photoreceptor responses revealed how such a synaptic architecture could serve to decorrelate signals from photoreceptor classes with overlapping opsin sensitivity, while keeping adequate information for the reconstruction of chromatic stimuli. This serves as an important first step towards understanding the computations underlying color vision on a cellular and synaptic level.

But what about Dm9 cells and skylight polarization? Surprisingly, unlike Dm8, Dm9 does not manifest any modality-specific morphology in the MEDRA, meaning that Dm9 cells located there appear to contact R7 and R8 photoreceptors from both DRA and non-DRA ommatidia (Fig. 5D) (Sancer et al., 2020). This is particularly interesting, since intra-ommatidial opponency has also been demonstrated in DRA photoreceptor terminals, resulting in polarization-opponent signals in both DRA.R7 and DRA.R8 terminals from the same ommatidium with their preferred polarization angles being orthogonal to each other (Weir et al., 2016). It is, therefore, possible that Dm9 cells in the DRA might mix color and polarization information in the photoreceptor terminals they innervate. Hence, color and skylight polarization information might already be integrated at this early stage in the visual circuit, as suggested by data from other insects (el Jundi et al., 2014). However, Dm9 crossing the DRA boundary do manifest specific differences in the localization of both pre- and post-synaptic membranes located within DRA columns as compared to those in non-DRA columns, hinting at possible differences in the synaptic connectivity within one cell (Sancer et al., 2020). For now, it therefore remains unknown whether Dm9 affects DRA photoreceptors and adjacent color-sensitive photoreceptor output and more studies are needed to answer this question.

5. Summary and outlook

The ability to distinguish colors and to navigate using the celestial pattern of polarized light is widespread across insect species living in very different habitats (Wehner, 2001). Interestingly, possible similarities between the underlying computations have been proposed (Labhart and Wehner, 2006), mostly based on electrophysiological data. For instance, a specific angle of polarization could be encoded via the relative excitation produced from tree groups of cells with different response properties (photoreceptor populations with different rhabdomere orientations), in analogy to color vision where different photoreceptor cell types express Rhodopsins with different chromatic sensitivities. Unfortunately, the response properties of large populations of polarization-sensitive circuit elements post-synaptic to DRA photoreceptors, like cricket polarization-opponent interneurons (Labhart, 1988), remain understudied across species. More recently, new data emerged supporting another previously proposed model, according to which the sum of DRA ommatidia form a 'matched filter' for the detection of skylight polarization pattern, at least in locusts (Zittrell et al., 2020). Things, therefore, become even more complicated, since it remains unknown whether color and skylight polarization are being processed via the same circuit mechanisms across species. Behavior experiments in different species clearly

show that one celestial cue can be ignored when another one is visible (Wehner, 2001; Dacke et al., 2020), raising the questions about species-specific adaptations. Although being a behavioral generalist, the molecular genetic and connectomic tools available in *Drosophila* promise to reveal differences and similarities between those circuits processing color versus skylight polarization at a cellular and synaptic level, providing a blueprint to which other insect species could be compared.

The neural circuit elements post-synaptic to *Drosophila* R7 and R8 photoreceptors, whose axons bypass the lamina neuropil, are crucial for processing color and polarized light signals. In recent years it became apparent that synaptic interconnections between photoreceptors themselves, as well as between their targets, result in rather complex properties of the photoreceptors. It is now crucial to extend the anatomical and physiological characterization of these circuits towards all cell types directly or indirectly post-synaptic to R7 and R8. Beyond Dm8 and Dm9, several synaptic targets of either R7, R8, or both have been reported (Takemura et al., 2008, 2015). However, significantly less is known about their physiological properties, as well as their relevance for guiding behavioral responses (Otsuna et al., 2014; Longden, 2018; Song and Lee, 2018; Schnaitmann et al., 2020). So far, most systematic dissection has focused on the circuits for detecting moving stimuli (Tuthill et al., 2013; Borst, 2014; Silies et al., 2014). The ongoing anatomical study of visual circuitry will greatly benefit from the recent publication of an electron microscopic dataset spanning the entire adult female fly brain (Zheng et al., 2018). Using these data, virtually any circuit can be reconstructed at synaptic resolution. Molecular genetic tools specifically labeling the newly identified cell types can then be retrieved from existing databases (Pfeiffer et al., 2008; Jenett et al., 2012), to be used for the physiological characterization, or manipulation in the behaving animal. Importantly, the same tools are currently being used to identify all the genes expressed by a particular optic lobe cell type, for instance neurotransmitters or their receptors (Davis et al., 2020), which in turn provides very useful information for understanding the computations they execute. Alternative approaches even aim at extracting such transcriptomes in an unbiased way from single cells, by collecting clusters of expression profiles, which must then be matched with their presumptive cell types (Konstantinides et al., 2018). Together with state-of-the art light microscopic techniques (Macpherson et al., 2015; Talay et al., 2017), as well as immunohistochemistry in combination with expansion microscopy (Wassie et al., 2019), these combined approaches will reveal crucial insight into both the similarities and differences of the anatomical structure of those neural circuits processing color versus polarized light. For example, it remains unknown to what extent the DRA region of the lamina neuropil (LADRA) also harbors modality-specific adaptations similar to what has been described for larger insects (el Jundi et al., 2014). The short visual fiber photoreceptors R1-6 terminating there have been shown to contribute to color vision (Schnaitmann et al., 2013), whereas a contribution to celestial polarization vision appears unlikely (Wernet et al., 2012). Nevertheless, modality-specific morphological specializations of R1-6 axons in the LADRA have been described in larger flies, where they form characteristic 'pseudo double cartridges' (Wunderer and Smola, 1982). The functional significance of this wiring pattern remains unknown.

In addition to studies on the structure and function of optic lobe cell types, the ongoing studies on both the development and the assembly of these neural circuits will provide crucial information that complements those datasets. For instance, the developmental origin of many lamina, medulla, and lobula cell types is currently being identified, thereby revealing their sibling relationship (neuroblast origin), as well as the transcriptional code and the mechanisms regulating the number and location of cell types (Li et al., 2013; Bertet et al., 2014; Chen et al., 2016; Erclik et al., 2017; Apitz and Salecker, 2018; Holguera and Desplan, 2018; Mora et al., 2018; Pinto-Teixeira et al., 2018). Transcriptomic data from specific cell types, collected at successive time points during development will reveal new transcription factors as well as the dynamic expression of cell surface molecules specifically expressed in any cell type of interest. Developmental studies will further clarify the exact role of adhesion molecules: Which ones act as specific cues for informing the formation of new synapses? Which ones are necessary for stabilizing transient synaptic connections? Which ones regulate the sorting of cell types during development? Which ones are necessary for inducing or suppressing apoptosis by mediating cell/cell contacts? Of particular importance are live imaging studies for revealing the dynamic nature of cell/cell interactions, as well as axon outgrowth and synaptic stabilization (Langen et al., 2015; Ozel et al., 2015).The growing number of studies related to these questions will reveal the common principles, as well as the cell type specific differences behind establishing specific synaptic connections. Finally, although visual input has been shown to play no significant role in the generation of synaptic specificity in the periphery of the fly visual system (Hiesinger et al., 2006), a recent study using genetically encoded indicators of activity during circuit assembly in the optic lobes revealed spontaneous activity waves in cell types that will be connected in the adult brain (Akin et al., 2019). Therefore, it turns out the combination of different tools (molecular biology, physiology, anatomy) bear the potential to provide answers on multiple aspects of neural circuit development and assembly, as well as adult circuit structure and function.

Author contributions

GS and MFW together planned the outline of text and figures. GS generated the figures. GS and MFW together wrote the manuscript. MFW acquired the funds.

Acknowledgments

The authors would like to thank the Wernet and Hiesinger Lab members for helpful suggestions on the manuscript. This work was supported by the Deutsche Forschungsgemeinschaft (DFG) through grants WE 5761/2-1, and SPP2205, through AFOSR grant FA9550-19-1-7005, through the Berlin Excellency Cluster NeuroCure, with support from the Fachbereich Biologie, Chemie & Pharmazie of the Freie Universität Berlin, as well as the Division of Neurobiology at Freie Universität Berlin.

References

Akin, O., Bajar, B.T., Keles, M.F., Frye, M.A., Zipursky, S.L., 2019. Cell-type-specific patterned stimulus-independent neuronal activity in the *Drosophila* visual system during synapse formation. Neuron 101 (5). https://doi.org/10.1016/j.neuron.2019.01.008, 894–904 e895.

Apitz, H., Salecker, I., 2018. Spatio-temporal relays control layer identity of direction-selective neuron subtypes in *Drosophila*. Nat. Commun. 9 (1), 2295. https://doi.org/10.1038/s41467-018-04592-z.

Bell, M.L., Earl, J.B., Britt, S.G., 2007. Two types of *Drosophila* R7 photoreceptor cells are arranged randomly: a model for stochastic cell-fate determination. J. Comp. Neurol. 502 (1), 75–85. https://doi.org/10.1002/cne.21298.

Bertet, C., Li, X., Erclik, T., Cavey, M., Wells, B., Desplan, C., 2014. Temporal patterning of neuroblasts controls Notch-mediated cell survival through regulation of hid or reaper. Cell 158 (5), 1173–1186. https://doi.org/10.1016/j.cell.2014.07.045.

Borst, A., 2014. In search of the Holy Grail of fly motion vision. Eur. J. Neurosci. 40 (9), 3285–3293. https://doi.org/10.1111/ejn.12731.

Carrillo, R.A., Ozkan, E., Menon, K.P., Nagarkar-Jaiswal, S., Lee, P.T., Jeon, M., et al., 2015. Control of synaptic connectivity by a network of *Drosophila* IgSF cell surface proteins. Cell 163 (7), 1770–1782. https://doi.org/10.1016/j.cell.2015.11.022.

Chen, Z., Del Valle Rodriguez, A., Li, X., Erclik, T., Fernandes, V.M., Desplan, C., 2016. A unique class of neural progenitors in the *Drosophila* optic lobe generates both migrating neurons and Glia. Cell Rep. 15 (4), 774–786. https://doi.org/10.1016/j.celrep.2016.03.061.

Chin, A.L., Lin, C.Y., Fu, T.F., Dickson, B.J., Chiang, A.S., 2014. Diversity and wiring variability of visual local neurons in the *Drosophila* medulla M6 stratum. J. Comp. Neurol. 522, 3795–3816.

Chou, W.H., Hall, K.J., Wilson, D.B., Wideman, C.L., Townson, S.M., Chadwell, L.V., Britt, S.G., 1996. Identification of a novel *Drosophila* opsin reveals specific patterning of the R7 and R8 photoreceptor cells. Neuron 17 (6), 1101–1115. https://doi.org/10.1016/s0896-6273(00)80243-3.

Chou, W.H., Huber, A., Bentrop, J., Schulz, S., Schwab, K., Chadwell, L.V., et al., 1999. Patterning of the R7 and R8 photoreceptor cells of *Drosophila*: evidence for induced and default cell-fate specification. Development 126 (4), 607–616. Retrieved from: http://www.ncbi.nlm.nih.gov/pubmed/9895309.

Courgeon, M., Desplan, C., 2019. Coordination between stochastic and deterministic specification in the *Drosophila* visual system. Science 366 (6463). https://doi.org/10.1126/science.aay6727.

Coyne, J.A., Boussy, I.A., Prout, T., Bryant, S.H., Jones, J.S., Moore, J.A., 1982. Long-distance migration of *Drosophila*. Am. Nat. 119, 589–595.

Coyne, J.A., Bryant, S.H., Turelli, M., 1987. Long-distance migration of *Drosophila*. 2. Presence in desolate sites and dispersal near a desert oasis. Am. Nat. 129, 847–861.

Dacke, M., Baird, E., el Jundi, B., Warrant, E.J., Byrne, M., 2020. How dung beetles steer straight. Annu. Rev. Entomol. https://doi.org/10.1146/annurev-ento-042020-102149.

Davis, F.P., Nern, A., Picard, S., Reiser, M.B., Rubin, G.M., Eddy, S.R., Henry, G.L., 2020. A genetic, genomic, and computational resource for exploring neural circuit function. Elife 9. https://doi.org/10.7554/eLife.50901.

Dickinson, M.H., 2014. Death Valley, *Drosophila*, and the Devonian toolkit. Annu. Rev. Entomol. 59, 51–72. https://doi.org/10.1146/annurev-ento-011613-162041.

el Jundi, B., Pfeiffer, K., Heinze, S., Homberg, U., 2014. Integration of polarization and chromatic cues in the insect sky compass. J. Comp. Physiol. A Neuroethol. Sens. Neural Behav. Physiol. 200 (6), 575–589. https://doi.org/10.1007/s00359-014-0890-6.

el Jundi, B., Pfeiffer, K., Homberg, U., 2011. A distinct layer of the medulla integrates sky compass signals in the brain of an insect. PLoS One 6 (11), e27855. https://doi.org/10.1371/journal.pone.0027855.

Erclik, T., Li, X., Courgeon, M., Bertet, C., Chen, Z., Baumert, R., et al., 2017. Integration of temporal and spatial patterning generates neural diversity. Nature 541 (7637), 365–370. https://doi.org/10.1038/nature20794.

Feiler, R., Bjornson, R., Kirschfeld, K., Mismer, D., Rubin, G.M., Smith, D.P., et al., 1992. Ectopic expression of ultraviolet-rhodopsins in the blue photoreceptor cells of *Drosophila*: visual physiology and photochemistry of transgenic animals. J. Neurosci. 12 (10), 3862–3868. Retrieved from: http://www.ncbi.nlm.nih.gov/pubmed/1403087.

Feinberg, E.H., Vanhoven, M.K., Bendesky, A., Wang, G., Fetter, R.D., Shen, K., Bargmann, C.I., 2008. GFP Reconstitution Across Synaptic Partners (GRASP) defines cell contacts and synapses in living nervous systems. Neuron 57 (3), 353–363. https://doi.org/10.1016/j.neuron.2007.11.030.

Fischbach, K.F., Dittrich, A.P.M., 1989. The optic lobe of *Drosophila melanogaster* .1. A Golgi analysis of wild-type structure. Cell Tissue Res. 258 (3), 441–475. Retrieved from: <Go to ISI>://WOS:A1989CC25600001.

Fortini, M.E., Rubin, G.M., 1990. Analysis of Cis-acting requirements of the Rh3 and Rh4 genes reveals a bipartite organization to rhodopsin promoters in *Drosophil melanogaster*. Genes Dev. 4 (3), 444–463. Retrieved from: <Go to ISI>://WOS:A1990DD09600013.

Fortini, M.E., Rubin, G.M., 1991. The optic lobe projection pattern of polarization-sensitive photoreceptor cells in *Drosophila melanogaster*. Cell Tissue Res. 265 (1), 185–191. Retrieved from: <Go to ISI>://WOS:A1991FU79300021.

Franceschini, N., Kirschfeld, K., Minke, B., 1981. Fluorescence of photoreceptor cells observed in vivo. Science 213 (4513), 1264–1267. Retrieved from: http://www.ncbi.nlm.nih.gov/pubmed/7268434.

Gao, S., Takemura, S.Y., Ting, C.Y., Huang, S., Lu, Z., Luan, H., et al., 2008. The neural substrate of spectral preference in *Drosophila*. Neuron 60 (2), 328–342. https://doi.org/10.1016/j.neuron.2008.08.010.

Heath, S.L., Christenson, M.P., Oriol, E., Saavedra-Weisenhaus, M., Kohn, J.R., Behnia, R., 2019. Circuit mechanisms underlying chromatic encoding in *Drosophila* photoreceptors. Curr. Biol. 30 (2) https://doi.org/10.1016/j.cub.2019.11.075, 264–275.e8.

Hiesinger, P.R., Zhai, R.G., Zhou, Y., Koh, T.W., Mehta, S.Q., Schulze, K.L., et al., 2006. Activity-independent prespecification of synaptic partners in the visual map of *Drosophila*. Curr. Biol. 16 (18), 1835–1843. https://doi.org/10.1016/j.cub.2006.07.047.

Hilbrant, M., Almudi, I., Leite, D.J., Kuncheria, L., Posnien, N., Nunes, M.D., McGregor, A.P., 2014. Sexual dimorphism and natural variation within and among species in the *Drosophila* retinal mosaic. BMC Evol. Biol. 14, 240. https://doi.org/10.1186/s12862-014-0240-x.

Holguera, I., Desplan, C., 2018. Neuronal specification in space and time. Science 362 (6411), 176–180. https://doi.org/10.1126/science.aas9435.

Huber, A., Schulz, S., Bentrop, J., Groell, C., Wolfrum, U., Paulsen, R., 1997. Molecular cloning of *Drosophila* Rh6 rhodopsin: the visual pigment of a subset of R8 photoreceptor cells. FEBS Lett. 406 (1–2), 6–10. https://doi.org/10.1016/s0014-5793(97)00210-x.

Ito, K., Shinomiya, K., Ito, M., Armstrong, J.D., Boyan, G., Hartenstein, V., Harzsch, S., Heisenberg, M., Homberg, U., Jenett, A., Keshishian, H., Restifo, L.L., Rössler, W., Simpson, J.H., Strausfeld, N.J., Strauss, R., Vosshall, L.B., Insect Brain Name Working Group, 2014. A systematic nomenclature for the insect brain. Neuron 81 (4), 755–765. https://doi.org/10.1016/j.neuron.2013.12.017.

Jenett, A., Rubin, G.M., Ngo, T.T., Shepherd, D., Murphy, C., Dionne, H., et al., 2012. A GAL4-driver line resource for *Drosophila* neurobiology. Cell Rep. 2 (4), 991–1001. https://doi.org/10.1016/j.celrep.2012.09.011.

Johnston Jr., R.J., Desplan, C., 2014. Interchromosomal communication coordinates intrinsically stochastic expression between alleles. Science 343 (6171), 661–665. https://doi.org/10.1126/science.1243039.

Jukam, D., Xie, B., Rister, J., Terrell, D., Charlton-Perkins, M., Pistillo, D., et al., 2013. Opposite feedbacks in the Hippo pathway for growth control and neural fate. Science 342 (6155), 1238016. https://doi.org/10.1126/science.1238016.

Karuppudurai, T., Lin, T.Y., Ting, C.Y., Pursley, R., Melnattur, K.V., Diao, F., et al., 2014. A hard-wired glutamatergic circuit pools and relays UV signals to mediate spectral preference in *Drosophila*. Neuron 81 (3), 603–615. https://doi.org/10.1016/j.neuron.2013.12.010.

Kind, E., Belušič, G., Wernet, M.F., 2020. Retinal Mosaics Across Fly Species: Variations on a Theme. In: Reference Module in Neuroscience and Biobehavioral Psychology. Elsevier.

Konstantinides, N., Kapuralin, K., Fadil, C., Barboza, L., Satija, R., Desplan, C., 2018. Phenotypic convergence: distinct transcription factors regulate common terminal features. Cell 174 (3). https://doi.org/10.1016/j.cell.2018.05.021, 622–635 e613.

Labhart, T., 1988. Polarization-opponent interneurons in the insect visual-system. Nature 331 (6155), 435–437. https://doi.org/10.1038/331435a0.

Labhart, T., Meyer, E.P., 1999. Detectors for polarized skylight in insects: a survey of ommatidial specializations in the dorsal rim area of the compound eye. Microsc. Res. Tech. 47 (6), 368–379. https://doi.org/10.1002/(SICI)1097-0029(19991215)47:6<368::AID-JEMT2>3.0.CO;2-Q.

Labhart, T., Wehner, R., 2006. Polarization vision. In: Warrant, E.J., Nilsson, D.E. (Eds.), Invertebrate Vision. Cambridge University Press, Cambridge, pp. 291–348.

Langen, M., Agi, E., Altschuler, D.J., Wu, L.F., Altschuler, S.J., Hiesinger, P.R., 2015. The developmental rules of neural superposition in *Drosophila*. Cell 162 (1), 120–133. https://doi.org/10.1016/j.cell.2015.05.055.

Li, X., Erclik, T., Bertet, C., Chen, Z., Voutev, R., Venkatesh, S., et al., 2013. Temporal patterning of *Drosophila* medulla neuroblasts controls neural fates. Nature 498 (7455), 456–462. https://doi.org/10.1038/nature12319.

Lin, T.Y., Luo, J., Shinomiya, K., Ting, C.Y., Lu, Z., Meinertzhagen, I.A., Lee, C.H., 2016. Mapping chromatic pathways in the *Drosophila* visual system. J. Comp. Neurol. 524 (2), 213–227. https://doi.org/10.1002/cne.23857.

Longden, K.D., 2018. Colour vision: a fresh view of lateral inhibition in *Drosophila*. Curr. Biol. 28 (7), R308–R311. https://doi.org/10.1016/j.cub.2018.02.052.

Luo, J., Ting, C.Y., Li, Y., McQueen, P., Lin, T.Y., Hsu, C.P., Lee, C.H., 2020. Antagonistic regulation by insulin-like peptide and activin ensures the elaboration of appropriate dendritic field sizes of amacrine neurons. Elife 9. https://doi.org/10.7554/eLife.50568.

Macpherson, L.J., Zaharieva, E.E., Kearney, P.J., Alpert, M.H., Lin, T.Y., Turan, Z., et al., 2015. Dynamic labelling of neural connections in multiple colours by trans-synaptic fluorescence complementation. Nat. Commun. 6, 10024. https://doi.org/10.1038/ncomms10024.

Mathejczyk, T.F., Wernet, M.F., 2017. Sensing Polarized Light in Insects. Oxford Encyclopedia of Neuroscience.

Mathejczyk, T.F., Wernet, M.F., 2019. Heading choices of flying *Drosophila* under changing angles of polarized light. Sci. Rep. 9 (1), 16773. https://doi.org/10.1038/s41598-019-53330-y.

Mathejczyk, T.F., Wernet, M.F., 2020. Modular assays for the quantitative study of visually guided navigation in both flying and walking flies. J. Neurosci. Methods 340, 108747. https://doi.org/10.1016/j.jneumeth.2020.108747.

Meinertzhagen, I., Hanson, T., 1993. The development of the optic lobe. In: Bate, M., Martinez-Arias, A. (Eds.), The Development of *Drosophila melanogaster*. Cold Spring Harbor Laboratory Press, New York, pp. 1363–1392.

Meinertzhagen, I.A., Takemura, S.Y., Lu, Z., Huang, S., Gao, S., Ting, C.Y., Lee, C.H., 2009. From form to function: the ways to know a neuron. J. Neurogenet. 23 (1–2), 68–77. https://doi.org/10.1080/01677060802610604.

Melnattur, K.V., Pursley, R., Lin, T.Y., Ting, C.Y., Smith, P.D., Pohida, T., Lee, C.H., 2014. Multiple redundant medulla projection neurons mediate color vision in *Drosophila*. J. Neurogenet. 28 (3–4), 374–388. https://doi.org/10.3109/01677063.2014.891590.

Menon, K.P., Kulkarni, V., Takemura, S.Y., Anaya, M., Zinn, K., 2019. Interactions between Dpr11 and DIP-gamma control selection of amacrine neurons in *Drosophila* color vision circuits. Elife 8. https://doi.org/10.7554/eLife.48935.

Mikeladze-Dvali, T., Wernet, M.F., Pistillo, D., Mazzoni, E.O., Teleman, A.A., Chen, Y.W., et al., 2005. The growth regulators warts/lats and melted interact in a bistable loop to specify opposite fates in *Drosophila* R8 photoreceptors. Cell 122 (5), 775–787. https://doi.org/10.1016/j.cell.2005.07.026.

Mora, N., Oliva, C., Fiers, M., Ejsmont, R., Soldano, A., Zhang, T.T., et al., 2018. A temporal transcriptional switch governs stem cell division, neuronal numbers, and maintenance of differentiation. Dev. Cell 45 (1). https://doi.org/10.1016/j.devcel.2018.02.023, 53–66 e55.

Nern, A., Pfeiffer, B.D., Rubin, G.M., 2015. Optimized tools for multicolor stochastic labeling reveal diverse stereotyped cell arrangements in the fly visual system. Proc. Natl. Acad. Sci. U. S. A. 112 (22), E2967–E2976. https://doi.org/10.1073/pnas.1506763112.

Otsuna, H., Shinomiya, K., Ito, K., 2014. Parallel neural pathways in higher visual centers of the *Drosophila* brain that mediate wavelength-specific behavior. Front. Neural Circuits 8, 8. https://doi.org/10.3389/fncir.2014.00008.

Ozel, M.N., Langen, M., Hassan, B.A., Hiesinger, P.R., 2015. Filopodial dynamics and growth cone stabilization in *Drosophila* visual circuit development. Elife 4. https://doi.org/10.7554/eLife.10721.

Papatsenko, D., Sheng, G., Desplan, C., 1997. A new rhodopsin in R8 photoreceptors of *Drosophila*: evidence for coordinate expression with Rh3 in R7 cells. Development 124 (9), 1665–1673. Retrieved from: http://www.ncbi.nlm.nih.gov/pubmed/9165115.

Perry, M., Kinoshita, M., Saldi, G., Huo, L., Arikawa, K., Desplan, C., 2016. Molecular logic behind the three-way stochastic choices that expand butterfly colour vision. Nature 535 (7611), 280. Retrieved from: <Go to ISI>://WOS:000379912600056.

Pfeiffer, B.D., Jenett, A., Hammonds, A.S., Ngo, T.T., Misra, S., Murphy, C., et al., 2008. Tools for neuroanatomy and neurogenetics in *Drosophila*. Proc. Natl. Acad. Sci. U. S. A. 105 (28), 9715–9720. https://doi.org/10.1073/pnas.0803697105.

Pinto-Teixeira, F., Koo, C., Rossi, A.M., Neriec, N., Bertet, C., Li, X., et al., 2018. Development of concurrent retinotopic maps in the fly motion detection circuit. Cell 173 (2). https://doi.org/10.1016/j.cell.2018.02.053, 485–498 e411.

Pollack, I., Hofbauer, A., 1991. Histamine-like immunoreactivity in the visual system and brain of *Drosophila melanogaster*. Cell Tissue Res. 266 (2), 391–398. https://doi.org/10.1007/bf00318195.

Salcedo, E., Huber, A., Henrich, S., Chadwell, L.V., Chou, W.H., Paulsen, R., Britt, S.G., 1999. Blue- and green-absorbing visual pigments of *Drosophila*: ectopic expression and physiological characterization of the R8 photoreceptor cell-specific Rh5 and Rh6 rhodopsins. J. Neurosci. 19 (24), 10716–10726. Retrieved from: http://www.ncbi.nlm.nih.gov/pubmed/10594055.

Sancer, G., Kind, E., Plazaola-Sasieta, H., Balke, J., Pham, T., Hasan, A., et al., 2019. Modality-specific circuits for skylight orientation in the fly visual system. Curr. Biol. https://doi.org/10.1016/j.cub.2019.07.020.

Sancer, G., Kind, E., Uhlhorn, J., Volkmann, J., Hammacher, J., Pham, T., et al., 2020. Cellular and synaptic adaptations of neural circuits processing skylight polarization in the fly. J. Comp. Physiol. A Neuroethol. Sens. Neural Behav. Physiol. 206 (2), 233–246. https://doi.org/10.1007/s00359-019-01389-3.

Schnaitmann, C., Garbers, C., Wachtler, T., Tanimoto, H., 2013. Color discrimination with broadband photoreceptors. Curr. Biol. 23 (23), 2375–2382. https://doi.org/10.1016/j.cub.2013.10.037.

Schnaitmann, C., Haikala, V., Abraham, E., Oberhauser, V., Thestrup, T., Griesbeck, O., Reiff, D.F., 2018. Color processing in the early visual system of *Drosophila*. Cell 172 (1–2). https://doi.org/10.1016/j.cell.2017.12.018, 318–330 e318.

Schnaitmann, C., Pagni, M., Reiff, D.F., 2020. Color vision in insects: insights from *Drosophila*. J. Comp. Physiol. A Neuroethol. Sens. Neural Behav. Physiol. 206 (2), 183–198. https://doi.org/10.1007/s00359-019-01397-3.

Silies, M., Gohl, D.M., Clandinin, T.R., 2014. Motion-detecting circuits in flies: coming into view. Annu. Rev. Neurosci. 37, 307–327. https://doi.org/10.1146/annurev-neuro-071013-013931.

Smola, U., Tscharntke, H., 1979. Twisted rhabdomeres in the dipteran eye. J. Comp. Physiol. 133 (4), 291–297. Retrieved from: <Go to ISI>://WOS:A1979HU30200005.

Song, B.M., Lee, C.H., 2018. Toward a mechanistic understanding of color vision in insects. Front. Neural Circuits 12, 16. https://doi.org/10.3389/fncir.2018.00016.

Stuart, A.E., 1999. From fruit flies to barnacles, histamine is the neurotransmitter of arthropod photoreceptors. Neuron 22 (3), 431–433. https://doi.org/10.1016/s0896-6273(00)80699-6.

Takemura, S., Bharioke, A., Lu, Z.Y., Nern, A., Vitaladevuni, S., Rivlin, P.K., et al., 2013. A visual motion detection circuit suggested by *Drosophila* connectomics. Nature 500 (7461), 175. Retrieved from: <Go to ISI>://WOS:000322825500028.

Takemura, S.Y., Lu, Z.Y., Meinertzhagen, I.A., 2008. Synaptic circuits of the *Drosophila* optic lobe: the input terminals to the medulla. J. Comp. Neurol. 509 (5), 493–513. Retrieved from: <Go to ISI>://WOS:000257630700003.

Takemura, S.Y., Xu, C.S., Lu, Z., Rivlin, P.K., Parag, T., Olbris, D.J., et al., 2015. Synaptic circuits and their variations within different columns in the visual system of *Drosophila*. Proc. Natl. Acad. Sci. U. S. A. 112 (44), 13711–13716. https://doi.org/10.1073/pnas.1509820112.

Talay, M., Richman, E.B., Snell, N.J., Hartmann, G.G., Fisher, J.D., Sorkac, A., et al., 2017. Transsynaptic mapping of second-order taste neurons in flies by trans-tango. Neuron 96 (4). https://doi.org/10.1016/j.neuron.2017.10.011, 783–795 e784.

Tan, L., Zhang, K.X., Pecot, M.Y., Nagarkar-Jaiswal, S., Lee, P.T., Takemura, S.Y., et al., 2015. Ig superfamily ligand and receptor pairs expressed in synaptic partners in *Drosophila*. Cell 163 (7), 1756–1769. https://doi.org/10.1016/j.cell.2015.11.021.

Ting, C.Y., Yonekura, S., Chung, P., Hsu, S.N., Robertson, H.M., Chiba, A., Lee, C.H., 2005. *Drosophila* N-cadherin functions in the first stage of the two-stage layer-selection process of R7 photoreceptor afferents. Development 132 (5), 953–963. https://doi.org/10.1242/dev.01661.

Ting, C.Y., McQueen, P.G., Pandya, N., Lin, T.Y., Yang, M., Reddy, O.V., et al., 2014. Photoreceptor-derived activin promotes dendritic termination and restricts the receptive fields of first-order interneurons in *Drosophila*. Neuron 81 (4), 830–846. https://doi.org/10.1016/j.neuron.2013.12.012.

Tomlinson, A., 2003. Patterning the peripheral retina of the fly: decoding a gradient. Dev. Cell 5 (5), 799–809. Retrieved from: http://www.ncbi.nlm.nih.gov/pubmed/14602079.

Tuthill, J.C., Nern, A., Holtz, S.L., Rubin, G.M., Reiser, M.B., 2013. Contributions of the 12 neuron classes in the fly lamina to motion vision. Neuron 79 (1), 128–140. https://doi.org/10.1016/j.neuron.2013.05.024.

Uhlhorn, J., Wernet, M.F., 2020. Colour vision: self-centered fly photoreceptors communicate over distances. Curr. Biol. 30 (2), R78–R81. https://doi.org/10.1016/j.cub.2019.11.050.

Velez, M.M., Gohl, D., Clandinin, T.R., Wernet, M.F., 2014a. Differences in neural circuitry guiding behavioral responses to polarized light presented to either the dorsal or ventral retina in *Drosophila*. J. Neurogenet. 28 (3–4), 348–360. https://doi.org/10.3109/01677063.2014.922556.

Velez, M.M., Wernet, M.F., Clark, D.A., Clandinin, T.R., 2014b. Walking *Drosophila* align with the e-vector of linearly polarized light through directed modulation of angular acceleration. J. Comp. Physiol. A Neuroethol. Sens. Neural Behav. Physiol. 200 (6), 603–614. https://doi.org/10.1007/s00359-014-0910-6.

Wada, S., 1974. Special marginal ommatidia of flies (Diptera-Brachycera) – architecture and distribution in compound eyes. Z. Morphol. Tiere 77 (2), 87–125. Retrieved from: <Go to ISI>://WOS:A1974S115800001.

Warren, T.L., Giraldo, Y.M., Dickinson, M.H., 2019. Celestial navigation in *Drosophila*. J. Exp. Biol. 222 (Pt Suppl. 1) https://doi.org/10.1242/jeb.186148.

Warren, T.L., Weir, P.T., Dickinson, M.H., 2018. Flying *Drosophila melanogaster* maintain arbitrary but stable headings relative to the angle of polarized light. J. Exp. Biol. 221 (Pt 9) https://doi.org/10.1242/jeb.177550.

Wassie, A.T., Zhao, Y., Boyden, E.S., 2019. Expansion microscopy: principles and uses in biological research. Nat. Methods 16 (1), 33–41. https://doi.org/10.1038/s41592-018-0219-4.

Wehner, R., 2001. Polarization vision–a uniform sensory capacity? J. Exp. Biol. 204 (Pt 14), 2589–2596.

Weir, P.T., Dickinson, M.H., 2012. Flying *Drosophila* orient to sky polarization. Curr. Biol. 22 (1), 21–27. Retrieved from: <Go to ISI>://WOS:000299144200017.

Weir, P.T., Henze, M.J., Bleul, C., Baumann-Klausener, F., Labhart, T., Dickinson, M.H., 2016. Anatomical reconstruction and functional imaging reveal an ordered array of skylight polarization detectors in *Drosophila*. J. Neurosci. 36 (19), 5397–5404. https://doi.org/10.1523/JNEUROSCI.0310-16.2016.

Wells, B.S., Pistillo, D., Barnhart, E., Desplan, C., 2017. Parallel activin and BMP signaling coordinates R7/R8 photoreceptor subtype pairing in the stochastic *Drosophila* retina. Elife 6. https://doi.org/10.7554/eLife.25301.

Wernet, M.F., Celik, A., Mikeladze-Dvali, T., Desplan, C., 2007. Generation of uniform fly retinas. Curr. Biol. 17 (23), R1002–R1003. https://doi.org/10.1016/j.cub.2007.10.006.

Wernet, M.F., Desplan, C., 2014. Homothorax and Extradenticle alter the transcription factor network in *Drosophila* ommatidia at the dorsal rim of the retina. Development 141 (4), 918–928. https://doi.org/10.1242/dev.103127.

Wernet, M.F., Labhart, T., Baumann, F., Mazzoni, E.O., Pichaud, F., Desplan, C., 2003. Homothorax switches function of *Drosophila* photoreceptors from color to polarized light sensors. Cell 115 (3), 267–279. Retrieved from: http://www.ncbi.nlm.nih.gov/pubmed/14636555.

Wernet, M.F., Mazzoni, E.O., Celik, A., Duncan, D.M., Duncan, I., Desplan, C., 2006. Stochastic spineless expression creates the retinal mosaic for colour vision. Nature 440 (7081), 174–180. https://doi.org/10.1038/nature04615.

Wernet, M.F., Meier, K.M., Baumann-Klausener, F., Dorfman, R., Weihe, U., Labhart, T., Desplan, C., 2014. Genetic dissection of photoreceptor subtype specification by the *Drosophila melanogaster* zinc finger proteins elbow and no ocelli. PLoS Genet. 10 (3), e1004210 https://doi.org/10.1371/journal.pgen.1004210.

Wernet, M.F., Perry, M.W., Desplan, C., 2015. The evolutionary diversity of insect retinal mosaics: common design principles and emerging molecular logic. Trends Genet. 31 (6), 316–328. https://doi.org/10.1016/j.tig.2015.04.006.

Wernet, M.F., Velez, M.M., Clark, D.A., Baumann-Klausener, F., Brown, J.R., Klovstad, M., et al., 2012. Genetic dissection reveals two separate retinal substrates for polarization vision in *Drosophila*. Curr. Biol. 22 (1), 12–20. https://doi.org/10.1016/j.cub.2011.11.028.

Wolf, R., Gebhardt, B., Gademann, R., Heisenberg, M., 1980. Polarization sensitivity of course control in *Drosophila melanogaster*. J. Comp. Physiol. 139 (3), 177–191. Retrieved from: <Go to ISI>://WOS:A1980KQ73100002.

Wu, M., Nern, A., Williamson, W.R., Morimoto, M.M., Reiser, M.B., Card, G.M., Rubin, G.M., 2016. Visual projection neurons in the *Drosophila* lobula link feature detection to distinct behavioral programs. Elife 5. https://doi.org/10.7554/eLife.21022.

Wunderer, H., Smola, U., 1982. Fine-structure of ommatidia at the dorsal eye margin of *Calliphora erythrocephala* Meigen (Diptera, Calliphoridae) – an eye region specialized for the detection of polarized-light. Int. J. Insect Morphol. Embryol. 11 (1), 25–38. Retrieved from: <Go to ISI>://WOS:A1982NG80400002.

Yamaguchi, S., Desplan, C., Heisenberg, M., 2010. Contribution of photoreceptor subtypes to spectral wavelength preference in *Drosophila*. Proc. Natl. Acad. Sci. U. S. A. 107 (12), 5634–5639. https://doi.org/10.1073/pnas.0809398107.

Zheng, Z., Lauritzen, J.S., Perlman, E., Robinson, C.G., Nichols, M., Milkie, D., et al., 2018. A complete electron microscopy volume of the brain of adult *Drosophila melanogaster*. Cell 174 (3). https://doi.org/10.1016/j.cell.2018.06.019, 730–743 e722.

Zittrell, F., Pfeiffer, K., Homberg, U., 2020. Matched-filter coding of sky polarization results in an internal sun compass in the brain of the desert locust. Proc. Natl. Acad. Sci. U. S. A., 202005192 https://doi.org/10.1073/pnas.2005192117.